Mechanics Based Design of Structures and Machines

ISSN: 1539-7734 (Print) 1539-7742 (Online) Journal homepage: https://www.tandfonline.com/loi/lmbd20

Second-Order Shear Deformation Theory to Analyze Stress Distribution for Solar Functionally Graded Plates#

A. Shahrjerdi , M. Bayat , F. Mustapha , S. M. Sapuan & R. Zahari

To cite this article: A. Shahrjerdi , M. Bayat , F. Mustapha , S. M. Sapuan & R. Zahari (2010) Second-Order Shear Deformation Theory to Analyze Stress Distribution for Solar Functionally Graded Plates# , Mechanics Based Design of Structures and Machines, 38:3, 348-361, DOI: 10.1080/15397731003744603

To link to this article: https://doi.org/10.1080/15397731003744603

Published online: 03 Aug 2010.

Mechanics Based Design of Structures and Machines, 38: 348–361, 2010

ISSN: 1539-7734 print/1539-7742 online
DOI: 10.1080/15397731003744603

SECOND-ORDER SHEAR DEFORMATION THEORY TO ANALYZE STRESS DISTRIBUTION FOR SOLAR FUNCTIONALLY GRADED PLATES[#]

A. Shahrjerdi[1], M. Bayat[1,2], F. Mustapha[3], S. M. Sapuan[1], and R. Zahari[3]

[1]*Department of Mechanical Engineering, Universiti Putra Malaysia, Selangor, Malaysia*
[2]*Institute of Advanced Technology, Universiti Putra Malaysia, Selangor, Malaysia*
[3]*Department of Aerospace Engineering, Universiti Putra Malaysia, Selangor, Malaysia*

Second-order shear deformation theory (SSDT) is applied to evaluate the displacement and stress fields of a solar functionally graded plate (SFGP) due to mechanical loadings. The material properties are graded by a simple power law between Full-ceramic and Full-metal at upper and lower surfaces, respectively. Navier's method is applied to find analytical results for derived equations by using energy method in case of simply supported boundary conditions. The effects of the material grading index of the plate on the stresses and displacements are investigated. It is revealed that the longitudinal stresses in the functionally graded (FG) plates lie between full-metal and full-ceramic plates. It is found that the neutral axes for SFGP move to upper surface and not at the mid-surface as predicted in the homogeneous plates. The SSDT has computed acceptable results for in-plane stresses and displacement fields when compared with the existing literatures.

Keywords: Second order shear deformation; Solar functionally graded plate; Stress analysis.

INTRODUCTION

Solar plate is used to focus solar radiation onto an absorber located at the focal point in parabolic dish concentrator to provide the solar energy. Concentrating solar collector consists of reflector over solar plate, the absorber and the housing. Parabolic disk is made from solar plates. The performance of a solar plate in terms efficiency, service life and optical alignment depends on the material and operating conditions. Normally, a solar plate can be fabricated from polished pure material or coated plate with some special cover (Howell and Bereny, 1979). However, for some specific application, such as in solar satellite, solar power tower and solar power heat engine can demand low weight and high temperature environment.

Received June 3, 2009; Accepted February 23, 2010
[#]Communicated by Z. Mroz.
Correspondence: F. Mustapha, Department of Aerospace Engineering, Universiti Putra Malaysia, 43400 UPM, Selangor, Malaysia; E-mail: Faizal@eng.upm.edu.my

High thermal resistance provides suitable stiffness to avoid unsought deformation to better optical alignment. Such plates need to be fabricated using special material such as a functionally graded material (FGM) with steel and ceramic combined together. It can be seen that compared to pure material plate, FGM plates of similar size give much lower weight and greater heat resistant. Also, a further weight reduction can be obtained by choosing suitable thickness profile for the solar plate. To be more specific, an solar functionally graded plate (SFGP) is analyzed for different FGM grading index and side to thickness ratio.

Plates have many practical engineering applications such as in steam and gas turbine rotors, turbo generators, internal combustion engines, casting ship propellers, turbojet engines, reciprocating and centrifugal compressors, heat furnaces and aerospace technology just to mention a few. Solar plate can be an example of plate in high temperature environment. To deal with this situation and prevent heat from being transferred to supports, the solar plate can be made of FGM with ceramic-rich at the upper surface and metal-rich at the lower surface. While the heat resistant property of the ceramic at the upper surface prevents heat from being transferred, the metal at the lower surface helps carry the stress due to the supported structure at the bottom surface.

Functionally graded materials are defined as combination of the two or more materials in the structure varying continuously as a function of position along certain dimension(s) of the structure (Reddy, 2000; Suresh and Mortensen, 1998). There are few researches on the stress and displacement analysis of functionally graded (FG) structures in contrary to the extensive investigations on isotropic and composite plates and shells as cited in Shao and Ma (2008), Yang and Munz (1997), Yang and Shen (2003), Ebrahimi et al. (2008), and Bayat et al. (2009).

Shear deformation theories have been applied to investigate the mechanical behaviour in FG structure. First-order shear deformation theory (FSDT) has been considered in several research such as Sahraee (2009), Sohn and Kim (2009), Bayat et al. (2008), and Prakash et al. (2009) just mention as a few. Praveen and Reddy (1998) studied the static and dynamic responses of FG ceramic-metal plate accounting for the transverse shear deformation, rotary inertia and moderately large rotations in the Von-Karman sense, in which effect of imposed temperature field on the response of the FG plate was discussed in detail.

Higher and third-order shear deformation theory (TSDT) was applied for FGMs structures by Matsunaga (2009), Ravikiran et al. (2008), Gilhooley et al. (2007), Chung and Chen (2007), Chi and Chung (2006), Ferreira et al. (2005), and references there in. Reddy and Cheng (2001) investigated three-dimensional thermomechanical deformations of simply supported, FG rectangular plates by using an asymptotic method. Higher order shear and normal deformable plate theory and a mesh-less method have been applied for Static deformations, free and forced vibrations of a thick rectangular FG elastic plate by Qian et al. (2004).

As mentioned above, shear deformation theories have been applied to consider transverse shear strains and rotation. Few studies have used second-order shear deformation theory (SSDT) as cited by Khdeir and Reddy (1999). They studied free vibration of laminated composite plates using SSDT. Bahtui and Eslami (2007) investigated the coupled thermoelastic response of a FG circular cylindrical shell by considering SSDT.

To the authors' knowledge, a few works have been done in the area of bending analysis of FGM plate by using SSDT. In this study, the displacement and stress components of SFGP are obtained based on SSDT. The material properties of solar plates are graded along the thickness direction according to a volume fraction power law distribution. Navier's method is applied to solve equations. This work aims to investigate the effect of material properties, side-to-thickness and aspect ratio for SFGP with simply support boundary conditions.

FG MATERIAL PROPERTIES

According to the power law distribution of the volume fraction, the material properties of the SFGP are function of out plane variable (Bayat et al., 2007)

$$\xi(x_3) = (\xi_c - \xi_m)(x_3/h + 1/2)^p + \xi_m, \tag{1}$$

where ξ_m and ξ_c represent the material property of the full-metal and full-ceramic plate, respectively; $-h/2 \leq x_3 \leq h/2$ is the thickness coordinate variable and h is the total thickness of the plate. $p \geq 0$ is the volume fraction exponent (also called grading index in this article);

$$(x_3/h + 1/2)^p \tag{2}$$

denotes the volume fraction of the ceramic.

SECOND-ORDER SHEAR DEFORMATION FORMULATIONS

It may be mentioned that although a ceramic-rich at the top surface and metal-rich at the bottom surface gradient has been considered for all the plates in this article, the method of solution that has been followed is independent of such a gradient and may be applied to other gradients as well. However, several applications considered in this article such as a SFGP to adjust the focal point justify consideration of metal-rich at bottom surface of the plates. To justify consideration of metal-rich at bottom surface of the plates the ductility and machine ability plays an important role. Also, for a SFGP thermal resistance plays an important role to make a good thermal resistance to avoid the deflection of the plate. Figure 1 shows a thin simply supported SFGP with constant thickness, h, width, a, and length, b, with Cartesian coordinate system (x_1, x_2, x_3).

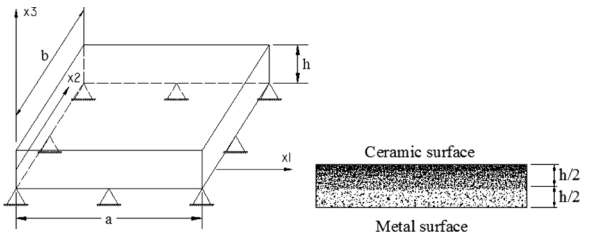

Figure 1 Simply supported boundary condition in SFGP.

Displacement and Stress–Strain Relations

The displacement field based on SSDT is given by Khdeir and Reddy (1999)

$$u_1 = u + x_3\phi_1 + x_3^2\phi_2, \quad u_2 = v + x_3\psi_1 + x_3^2\psi_2, \quad u_3 = w, \tag{3}$$

where (u_1, u_2, u_3) are the displacements in the (x_1, x_2, x_3) directions, respectively; (u, v, w) are displacement of mid-plane. All displacement components are functions of position (x_1, x_2) and time t, but for brevity, all displacement components represent by $(u, v, w, \phi_1, \phi_2, \psi_1, \psi_2)$. A comma represents the differentiation to the space.

The strain–displacement equations of the linear strain are given in Reddy (2007)

$$\{\varepsilon_{11}, \varepsilon_{22}, \varepsilon_{12}\} = \{\varepsilon_{11}^0, \varepsilon_{22}^0, \varepsilon_{12}^0\} + x_3\{\kappa_{11}, \kappa_{22}, \kappa_{12}\} + x_3^2\{\kappa'_{11}, \kappa'_{22}, \kappa'_{12}\} \tag{4a}$$

$$\{\gamma_{23}, \gamma_{13}\} = \{\gamma_{23}^0, \gamma_{13}^0\} + x_3\{\gamma_{23}^1, \gamma_{13}^1\}, \tag{4b}$$

where

$$\begin{aligned}
&\varepsilon_{11}^0 = u_{,x_1}; \quad \kappa_{11} = \phi_{1,x_1}; \quad \kappa'_{11} = \phi_{2,x_2}; \quad \varepsilon_{22}^0 = v_{,x_2}; \quad \kappa_{22} = \psi_{1,x_2}; \quad \kappa'_{22} = \psi_{2,x_2};\\
&\varepsilon_{12}^0 = u_{,x_2} + v_{,x_1}\ \kappa_{12} = \phi_{1,x_2} + \psi_{1,x_1}; \quad \kappa'_{12} = \phi_{2,x_2} + \psi_{2,x_1};\\
&\gamma_{23}^0 = \psi_1 + w_{,x_2}; \quad \gamma_{13}^0 = \phi_1 + w_{,x_1}; \quad \gamma_{23}^1 = 2\psi_2; \quad \gamma_{13}^1 = 2\phi_2.
\end{aligned} \tag{5}$$

The strains of the middle surface, $(\varepsilon_{11}^0, \varepsilon_{22}^0, \varepsilon_{12}^0)$, are called the membrane strains, and (k_{11}, k_{22}, k_{12}) are the flexural (bending) strains (Reddy, 2007).

The stress–strain relations are given in Khdeir and Reddy (1999)

$$\begin{Bmatrix} \sigma_{11} \\ \sigma_{22} \\ \sigma_{23} \\ \sigma_{13} \\ \sigma_{12} \end{Bmatrix} = \begin{Bmatrix} q_{11} & q_{12} & 0 & 0 & 0 \\ q_{12} & q_{22} & 0 & 0 & 0 \\ 0 & 0 & q_{44} & 0 & 0 \\ 0 & 0 & 0 & q_{55} & 0 \\ 0 & 0 & 0 & 0 & q_{66} \end{Bmatrix} \begin{Bmatrix} \varepsilon_{11} \\ \varepsilon_{22} \\ \gamma_{23} \\ \gamma_{13} \\ \varepsilon_{12} \end{Bmatrix}, \tag{6}$$

where q_{ij} are the transformed reduced stiffness defined by

$$q_{11} = q_{22} = E(x_3)/1 - v^2 \quad q_{12} = vq_{11} \quad q_{44} = q_{55} = q_{66} = E(x_3)/2(1 + v). \tag{7}$$

Equilibrium Equations

For a SFGP, K, U, and V are the kinetic, strain, and potential energies of the plate, respectively. The summation of the potential energy of external forces and strain energy, $U + V$, is called the total potential energy, Π, of the body. The Hamilton's principle for an elastic body can be represented by Reddy (2007),

$$\int_{t_1}^{t_2} (\delta K - \delta\Pi)dt = 0. \tag{8}$$

The inertias are defined as

$$I_i = \int_{\frac{-h}{2}}^{\frac{h}{2}} \rho(x_3)^i dx_3 \quad (i = 0, 1, 2, \ldots, 6), \tag{9}$$

where ρ is density of the SFGP that follow the power law distribution. Hamilton's principle, Equation (8), by considering the displacement field based on SSDT, Equation (3), yields the complete form of the governing equations:

$$\begin{aligned}
&N_{11,x_1}+N_{12,x_2} = I_0\ddot{u}+I_2\ddot{\phi}_2+I_1\ddot{\phi}_1; && N_{22,x_2}+N_{12,x_1} = I_0\ddot{v}+I_2\ddot{\psi}_2+I_1\ddot{\psi}_1\\
&Q_{13,x_1}+Q_{23,x_2}+q(x_1, x_2) = I_0\ddot{w}; && M_{11,x_1}+M_{12,x_2} - Q_{13} = I_2\ddot{\phi}_1+I_1\ddot{u}+I_3\ddot{\phi}_2\\
&L_{11,x_1}+L_{12,x_2} - 2R_{13} = I_2\ddot{u}+I_4\ddot{\phi}_2+I_3\ddot{\phi}_1; && M_{22,x_2}+M_{12,x_1} - Q_{23} = I_2\ddot{\psi}_1+I_1\ddot{v}+I_3\ddot{\psi}_2\\
&L_{22,x_2}+L_{12,x_1} - 2R_{23} = I_2\ddot{v}+I_4\ddot{\psi}_2+I_3\ddot{\psi}_1,
\end{aligned} \tag{10}$$

where N, M, L, Q and R are the stress resultants for a SFGP. These parameters are defined as:

$$\begin{Bmatrix} \{N\} \\ \{M\} \\ \{L\} \end{Bmatrix} = \begin{bmatrix} [A] & [B] & [D] \\ [B] & [D] & [E] \\ [D] & [E] & [F] \end{bmatrix} \begin{Bmatrix} \{\varepsilon^0\} \\ \{\kappa\} \\ \{\kappa'\} \end{Bmatrix}, \quad \begin{Bmatrix} \{Q\} \\ \{R\} \end{Bmatrix} = \begin{bmatrix} [A] & [B] \\ [B] & [D] \end{bmatrix} \begin{Bmatrix} \{\gamma^0\} \\ \{\gamma^1\} \end{Bmatrix}, \tag{11}$$

where

$$\begin{aligned}
A_{ij}, B_{ij}, D_{ij}, E_{ij}, F_{ij} = &\int_{\frac{-h}{2}}^{\frac{h}{2}} q_{ij}\left(1, x_3, x_3^2, x_3^3, x_3^4\right) dx_3;\\
&\times \begin{cases} A_{ij}, D_{ij}, F_{ij} & (i, j = 1, 2, 4, 5, 6) \\ E_{ij}, B_{ij} & (i, j = 1, 2, 6) \end{cases},
\end{aligned} \tag{12}$$

where A_{ij}, B_{ij}, D_{ij}, E_{ij}, and F_{ij} are SFGP stiffness.

Navier's equations for FG plates are obtained by substituting Equations (5) and (12) into (11) and then in equation (10) as follow:

$$\begin{aligned}
&A_{11}u_{,x_1x_1} + A_{66}u_{,x_2x_2} + (A_{12} + A_{66})\, v_{,x_1x_2} + B_{11}\phi_{1,x_1x_1} + B_{66}\phi_{1,x_2x_2} + D_{11}\phi_{2,x_1x_1}\\
&\quad + D_{66}\phi_{2,x_2x_2} + (B_{12} + B_{66})\,\psi_{1,x_1x_2} + (D_{12} + D_{66})\,\psi_{2,x_1x_2} = I_0\ddot{u} + I_2\ddot{\phi}_2 + I_1\ddot{\phi}_1
\end{aligned} \tag{13a}$$

$$\begin{aligned}
&(A_{12} + A_{66})u_{,x_1x_2} + A_{22}v_{,x_2x_2} + A_{66}v_{,x_1x_1} + (B_{12} + B_{66})\phi_{1,x_1x_2} + (D_{12} + D_{66})\phi_{2,x_1x_2}\\
&\quad + B_{66}\psi_{1,x_1x_1} + B_{22}\psi_{1,x_2x_2} + D_{66}\psi_{2,x_1x_1} + D_{22}\psi_{2,x_2x_2} = I_0\ddot{v} + I_2\ddot{\psi}_2 + I_1\ddot{\psi}_1
\end{aligned} \tag{13b}$$

$$\begin{aligned}
&A_{55}\phi_{1,x_1} + A_{55}w_{,x_1x_1} + 2B_{55}\phi_{2,x_1} + A_{44}\psi_{1,x_2} + A_{44}w_{,x_2x_2} + 2B_{44}\psi_{2,x_2}\\
&\quad + q(x_1, x_2) = I_0\ddot{w}
\end{aligned} \tag{13c}$$

$$\begin{aligned}
&B_{11}u_{,x_1x_1} + B_{66}u_{,x_2x_2} + (B_{12} + B_{66})\, v_{,x_1x_2} + D_{11}\phi_{1,x_1x_1} + D_{66}\phi_{1,x_1x_2}\\
&\quad + E_{11}\phi_{2,x_1x_1} + E_{66}\phi_{2,x_2x_2} + (D_{12} + D_{66})\,\psi_{1,x_1x_2} + (E_{12} + E_{66})\,\psi_{2,x_1x_2}\\
&\quad - A_{55}w_{,x_1} - A_{55}\phi_1 - 2B_{55}\phi_2 = I_2\ddot{\phi}_1 + I_1\ddot{u} + I_3\ddot{\phi}_2
\end{aligned} \tag{13d}$$

$$D_{11}u_{,x_1x_1}+D_{66}u_{,x_2x_2}+D_{12}v_{,x_1x_2}+E_{11}\phi_{1,x_1x_1}+E_{66}\phi_{1,x_2x_2}+F_{11}\phi_{2,x_1x_1}+F_{66}\phi_{2,x_2x_2}$$
$$+(E_{12}+E_{66})\psi_{1,x_1x_2}+(F_{12}+F_{66})\psi_{2,x_1x_2}-2\left(B_{55}w_{,x_1}+2D_{55}\phi_2+B_{55}\phi_1\right)$$
$$=I_2\ddot{u}+I_4\ddot{\phi}_2+I_3\ddot{\phi}_1 \tag{13e}$$

$$(B_{12}+B_{66})u_{,x_1x_2}+B_{22}v_{,x_1x_1}+B_{66}v_{,x_2x_2}-A_{44}w_{,x_2}+(D_{12}+D_{66})\phi_{1,x_1x_2}$$
$$+(E_{12}+E_{66})\phi_{2,x_1x_2}+D_{66}\psi_{1,x_1x_1}+D_{22}\psi_{1,x_2x_2}+E_{66}\psi_{2,x_1x_1}$$
$$+E_{22}\psi_{2,x_2x_2}-A_{44}\psi_1-2B_{44}\psi_2=I_2\ddot{\psi}_1+I_1\ddot{v}+I_3\ddot{\psi}_2 \tag{13f}$$

$$(D_{12}+D_{66})u_{,x_1x_2}+D_{66}v_{,x_1x_1}+D_{22}v_{,x_2x_2}-2B_{44}w_{,x_2}+(E_{12}+E_{66})\phi_{1,x_1x_2}$$
$$+(F_{12}+F_{66})\phi_{2,x_1x_2}+E_{66}\psi_{1,x_1x_1}+E_{22}\psi_{1,x_2x_2}+F_{66}\psi_2,x_1x_1+F_{22}\psi_2,$$
$$\times x_2x_2-2B_{44}\psi_1-4D_{44}\psi_2=I_2\ddot{v}+I_4\ddot{\psi}_2+I_3\ddot{\psi}_1. \tag{13g}$$

It can be noted that by considering zero value for ϕ_2 and ψ_2 in equilibrium Equations (10) and Navier's Equations (13), FSDT equations can be obtained such as Reddy (2007).

BOUNDARY CONDITIONS

Edges Boundary Conditions

The solutions of the governing equations of motion (13) under following simply supported boundary conditions must be satisfied

$$x_1=0,\quad a\Rightarrow\{v,w,\psi_1,\psi_2,M_{11},N_{11}=0\}\quad\text{and}$$
$$x_2=0,\quad b\Rightarrow\{u,w,\phi_1,\phi_2,M_{22},N_{22}=0\}. \tag{14}$$

Surface Applied Loads

A SFGP subjected to the lateral load $q_{x_3}(x_1,x_2)$ at top surface. The lateral load can be defined as

$$q(x_1,x_2)=\sum_{n=1}^{\infty}\sum_{m=1}^{\infty}q_{mn}\sin\alpha x_1\sin\beta x_2, \tag{15a}$$

where $\alpha=m\pi/a$, $\beta=n\pi/b$,

$$q_{mn}=\int\int q(x_1,x_2)\sin\alpha x_1\sin\beta x_2dx_1\,dx_2. \tag{15b}$$

Sinusoidal and uniform loads are considered (Zenkour, 2006)

1-Sinusoidal load (SL): $q(x_1,x_2)=q_0\sin\alpha x_1\sin\beta x_2,\quad m=n=1$ and $q_{11}=q_0$

2-Uniform load (UL): $q(x_1,x_2)=q_0,\quad q_{mn}=\dfrac{16q_0}{\pi^2mn}:m,n=1,3,5,\ldots,$

$$q_{mn}=0:m,n=2,4,6,\ldots$$

METHODOLOGY

Navier's method is used for solution of governing Equations (13). In Navier's method, the displacement components and mechanical loads (Eq. (15a)) are expanded in trigonometric series (Reddy, 2007; Zenkour, 2007)

$$\{u, \phi_1, \phi_2\} = \sum\sum \{u_{mn}(t), \phi_{1mn}(t), \phi_{2mn}(t)\} \cos \alpha x_1 \sin \beta x_2 \tag{16a}$$

$$\{v, \psi_1, \psi_2\} = \sum\sum \{v_{mn}(t), \psi_{1mn}(t), \psi_{2mn}(t)\} \sin \alpha x_1 \cos \beta x_2;$$

$$w = \sum_{n=1}^{\infty}\sum_{m=1}^{\infty} w_{mn}(t) \sin \alpha x_1 \sin \beta x_2. \tag{16b}$$

The static solution can be obtained from substituting Equation (16) into Navier's Equation (13), by setting the time derivative terms to zero

$$[C] \quad \{u_{mn} \quad v_{mn} \quad w_{mn} \quad \phi_{1mn} \quad \phi_{2mn} \quad \psi_{1mn} \quad \psi_{2mn}\}^T = \{0 \quad 0 \quad q(x_1, x_2) \quad 0 \quad 0 \quad 0 \quad 0\}^T, \tag{17}$$

where

$$C_{11} = A_{11}\alpha^2 + A_{66}\beta^2; \quad C_{12} = (A_{12} + A_{66})\alpha\beta; \quad C_{13} = 0; \quad C_{14} = B_{11}\alpha^2 + B_{66}\beta^2$$
$$C_{15} = D_{11}\alpha^2 + D_{66}\beta^2; \quad C_{16} = (B_{12} + B_{66})\alpha\beta; \quad C_{17} = (D_{12} + D_{66})\alpha\beta \tag{18}$$

$$C_{21} = C_{12}; \quad C_{22} = A_{66}\alpha^2 + A_{22}\beta^2; \quad C_{23} = 0; \quad C_{24} = (B_{12} + B_{66})\alpha\beta;$$
$$C_{25} = (D_{12} + D_{66})\alpha\beta; \quad C_{26} = B_{66}\alpha^2 + B_{22}\beta^2; \quad C_{27} = D_{66}\alpha^2 + D_{22}\beta^2$$

$$C_{31} = C_{13}; \quad C_{32} = C_{23}; \quad C_{33} = A_{55}\alpha^2 + A_{44}\beta^2; \quad C_{34} = A_{55}\alpha; \quad C_{35} = 2B_{55}\alpha;$$
$$C_{36} = A_{44}\beta; \quad C_{37} = 2B_{44}\beta$$

$$C_{41} = C_{14}; \quad C_{42} = C_{24}; \quad C_{43} = C_{34}; \quad C_{44} = D_{11}\alpha^2 + D_{66}\beta^2 + A_{55};$$
$$C_{45} = E_{11}\alpha^2 + E_{66}\beta^2 + 2B_{55}. \quad C_{46} = (D_{12} + D_{66})\alpha\beta; \quad C_{47} = (E_{12} + E_{66})\alpha\beta$$

$$C_{51} = C_{15}; \quad C_{52} = C_{25}; \quad C_{53} = C_{35}; \quad C_{54} = C_{45}; \quad C_{55} = F_{11}\alpha^2 + F_{66}\beta^2 + 4D_{55};$$
$$C_{56} = (E_{12} + E_{66})\alpha\beta; \quad C_{57} = (F_{12} + F_{66})\alpha\beta$$

$$C_{61} = C_{16}; \quad C_{62} = C_{26}; \quad C_{63} = C_{36}; \quad C_{64} = C_{46}; \quad C_{65} = C_{56};$$
$$C_{66} = D_{66}\alpha^2 + D_{22}\beta^2 + A_{44}; \quad C_{67} = E_{66}\alpha^2 + E_{22}\beta^2 + 2B_{44}$$

$$C_{71} = C_{17}; \quad C_{72} = C_{27}; \quad C_{73} = C_{37}; \quad C_{74} = C_{47}; C_{75} = C_{57}; \quad C_{76} = C_{67};$$
$$C_{77} = F_{66}\alpha^2 + F_{22}\beta^2 + 4D_{44}.$$

Substituting Equation (18) into Equation (17) for each value of $m, n = 1, 2, 3, \ldots$ gives $(u_{mn}, v_{mn}, w_{mn}, \phi_{1mm}, \phi_{2mn}, \psi_{1mn}, \psi_{2mn})$ which can then be used to compute the displacement field.

For the bending case the in-plane stresses and transverse shear stresses can be computed by using the displacement components (Eq. (16)) into Equation (5) and then into Equation (7), the stress field shows as:

$$\sigma_{11} = -\begin{bmatrix} \sum_{n=1}^{\infty}\sum_{m=1}^{\infty}(\alpha q_{11}u_{mn} + \beta q_{12}v_{mn}) \\ + x_3\sum_{n=1}^{\infty}\sum_{m=1}^{\infty}(\alpha q_{11}\phi_{1mn} + \beta q_{12}\psi_{1mn}) \\ + x_3^2\sum_{n=1}^{\infty}\sum_{m=1}^{\infty}(\alpha q_{11}\phi_{2mn} + \beta q_{12}\psi_{2mn}) \end{bmatrix} \sin\alpha x_1 \sin\beta x_2 \tag{19a}$$

$$\sigma_{22} = -\begin{bmatrix} \sum_{n=1}^{\infty}\sum_{m=1}^{\infty}(\alpha q_{12}u_{mn} + \beta q_{22}v_{mn}) \\ + x_3\sum_{n=1}^{\infty}\sum_{m=1}^{\infty}(\alpha q_{12}\phi_{1mn} + \beta q_{22}\psi_{1mn}) \\ + x_3^2\sum_{n=1}^{\infty}\sum_{m=1}^{\infty}(\alpha q_{12}\phi_{2mn} + \beta q_{22}\psi_{2mn}) \end{bmatrix} \sin\alpha x_1 \sin\beta x_2 \tag{19b}$$

$$\sigma_{12} = \begin{bmatrix} \sum_{n=1}^{\infty}\sum_{m=1}^{\infty}(\beta q_{66}u_{mn} + \alpha q_{66}v_{mn}) \\ + x_3\sum_{n=1}^{\infty}\sum_{m=1}^{\infty}(\beta q_{66}\phi_{1mn} + \alpha q_{66}\psi_{1mn}) \\ + x_3^2\sum_{n=1}^{\infty}\sum_{m=1}^{\infty}(\beta q_{66}\phi_{2mn} + \alpha q_{66}\psi_{2mn}) \end{bmatrix} \cos\alpha x_1 \cos\beta x_2 \tag{19c}$$

VERIFICATION AND NUMERICAL EXAMPLES

Verification

For the verification of the results, the numerical method for FG reported by Zenkour (2006) is considered. Zenkour (2006) illustrated displacement field in FG square plate by considering sinusoidal and uniform distributed loads when $E_{Metal} = 70GPa$, $E_{Ceramic} = 380GPa$ and $v = 0.3$ that are shown in Table 1.

In Table 1, a SFGP consisting of aluminum and alumina is considered. Nondimensional displacements and stresses are presented according to Table 2 in Zenkour (2006).

Table 1 presents the effect of grading index p on the nondimensional displacement and stress fields in a SFGP ($a/h = 10$). Two types of loads such as SL and UL are considered. It can be observed that the results due to UL in comparison with SL always over-predict the value of displacements and stresses. It is seen that the vertical displacement ($\bar{w}$) and $\bar{\sigma}_{11}$ increase by increasing the value of grading index p. It is also seen that stress field for full-ceramic and full-metal plate is the same.

Numerical Example

The dimensionless analysis has been done by considering material properties that reported in Table 2 (Bayat et al., 2007).

It can be noted the solution of trigonometric shear deformation plate theory (FSDT and TSDT) for FG plates are available in the literature, to the emphasis on SSDT, we restrict our attention to SSDT theory for square plates under different cases of loads. The results in figures for in-plane stresses are obtained at center of plate $(a/2, b/2)$ and for in-plane shear stress are presented for $(a/2, b/2)$ and $(0, 0)$. Displacement results also are obtained in $(a/2, b/2)$. In figures nondimensional

Table 1 Nondimensional displacements and stresses by applying sinusoidal and uniform distributed loads for different values of grading index (p)

loading	p	$\bar{u}_1$	$\bar{u}_2$	$\bar{w}$	$\bar{\sigma}_{11}$	$\bar{\sigma}_{22}$	$\bar{\sigma}_{12}$
S.L. (Present work)	Ceramic	0.2201	0.1467	0.2934	1.9757	1.3171	0.7092
S.L. Ref (Zenkour, 2006)	Ceramic	0.2309	0.1539	0.2960	1.9955	1.3121	0.7065
U.L. (Present work)	Ceramic	0.3568	0.2378	0.4756	3.2029	2.1353	1.1497
U.L. Ref (Zenkour, 2006)	Ceramic	0.3904	0.2603	0.4665	2.8932	1.9101	1.2850
S.L. (Present work)	1	0.6438	0.4979	0.5856	3.0702	1.4972	0.6107
S.L. Ref (Zenkour, 2006)	1	0.6626	0.5093	0.5889	3.0870	1.4894	0.6110
U.L. (Present work)	1	1.0437	0.8072	0.9494	4.9773	2.4272	0.9901
U.L. Ref (Zenkour, 2006)	1	1.1153	0.8566	0.9287	4.4745	2.1692	1.1143
S.L. (Present work)	5	1.0755	0.8557	0.8979	4.2203	1.1147	0.5765
S.L. Ref (Zenkour, 2006)	5	1.1158	0.8792	0.9118	4.2488	1.1029	0.5755
U.L. (Present work)	5	1.7436	1.3872	1.4557	6.8417	1.8072	0.9346
U.L. Ref (Zenkour, 2006)	5	1.8820	1.4809	1.4356	6.1504	1.6104	1.0451
S.L. (Present work)	10	1.0869	0.8445	0.9890	5.0439	0.8890	0.5914
S.L. Ref (Zenkour, 2006)	10	1.1372	0.8756	1.0089	5.0890	0.8775	0.5894
U.L. (Present work)	10	1.7620	1.3690	1.6034	8.1770	1.4412	0.9587
U.L. Ref (Zenkour, 2006)	10	1.9217	1.4778	1.5876	7.3689	1.2820	1.0694
S.L. (Present work)	Metal	1.1949	0.7966	1.5929	1.9757	1.3171	0.7092
S.L. Ref (Zenkour, 2006)	Metal	1.2534	0.8356	1.6070	1.9955	1.3121	0.7065
U.L. (Present work)	Metal	1.9371	1.2914	2.5823	3.2029	2.1353	1.1497
U.L. Ref (Zenkour, 2006)	Metal	2.1194	1.4129	2.5327	2.8932	1.9103	1.2850

displacements and stresses for aluminum and zirconia or alumina are considered under UL according to the following definitions:

$$\bar{w} = w_0(10 \times h^3 \times E_c/a^4 q_0); \quad \{\bar{u}_1, \bar{u}_2\} = \{u_1, u_2\}\,(100 \times h^3 \times E_c/a^4 q_0);$$
$$\times \{\bar{\sigma}_{11}, \bar{\sigma}_{22}, \bar{\sigma}_{12}\} = \{\sigma_{11}, \sigma_{22}, \sigma_{12}\}\,(h/aq_0).$$

The nondimensional in-plane stresses ($\bar{\sigma}_{11}$) in SFGP for different values of grading index (p) and side-to-thickness ratio (a/h) are shown in Figure 2.

$\bar{\sigma}_{11}$ in full-ceramic ($p = 0.0$) is smaller than it for other SFGP due to higher value of Young modules in ceramic. It is seen that dimensionless longitudinal stress increases with the increase of the grading index and the results in SFGP are between full-ceramic ($p = 0.0$) and full-metal plate ($p \to \infty$). As expected when side-to-thickness (a/h) ratio increases the in-plane stresses increase because of the reducing stiffness.

Table 2 Material properties used in the numerical example and validation

Material property	E (Gpa)	v
Zirconia, Ceramic	211.0	0.33
Aluminum, Metal	68.9	0.33

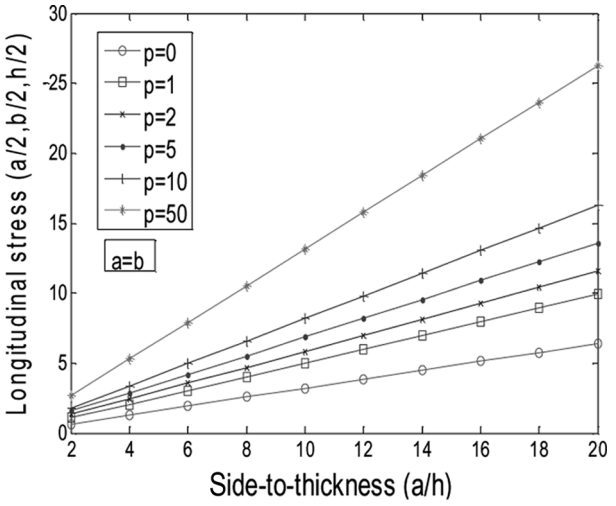

Figure 2 Nondimensional longitudinal stress distributions of SFGP versus side-to-thickness (a/h) for different values of grading index (p) under uniformly distributed load.

The variation of longitudinal stress through the thickness of SFGP for different values of grading index (p) under uniformly distributed load are presented in Figure 3.

As expected, the neutral axis for pure material plates is at $x_3 = 0.0$, while the neutral axis for SFGP moves to upper surface. It can be seen longitudinal stresses (σ_{11}) follow harmonic function for SFGP whereas it is linear for pure material plates. This is clearly that the maximum compressive stresses occur at lower surface and the maximum tensile stresses occur at upper surface.

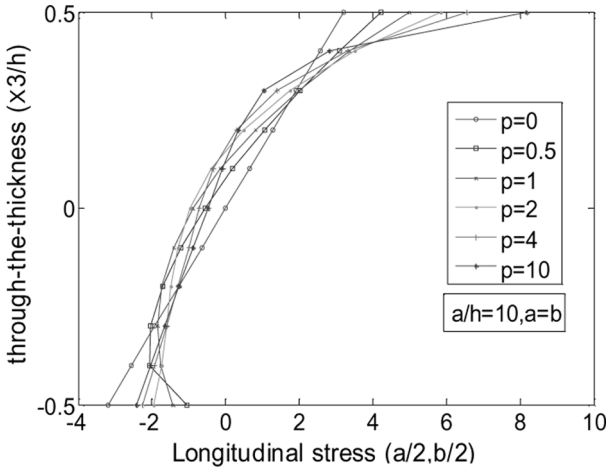

Figure 3 Nondimensional longitudinal stress distributions of SFGP through the thickness ratio (x_3/h) for different values of grading index (p) under uniformly distributed load.

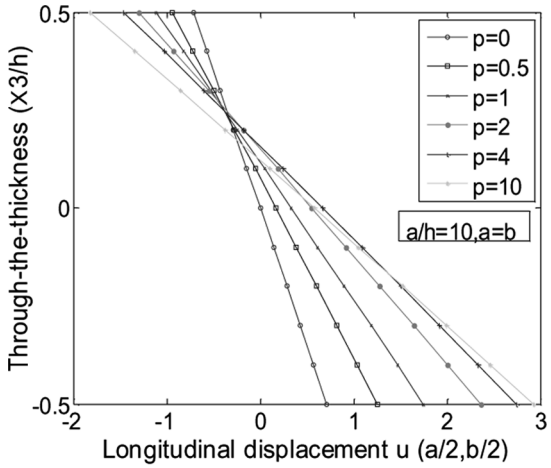

Figure 4 Nondimensional longitudinal displacement ($\bar{u}_1$) through the thickness (x_3/h) of SFGP for different values of grading index (p) under uniformly distributed load.

The results obtained by SSDT in this study is similar to the results have been obtained by third order shear deformation as reported in Matsunaga (2009).

The dimensionless displacement in $x_1(u_1)$ direction through the thickness (x_3/h) is demonstrated for different values of grading index (p) in Figure 4.

Figure 4 illustrates that the variation of displacement (u_1) is linear through the thickness. As it is expected the values of the displacement (u_1) in full metal is greater than those in full ceramic.

Figure 5 depicts the nondimensional transverse displacement (u_2) versus aspect out plane variation (x_3/h) for different values of grading index (p).

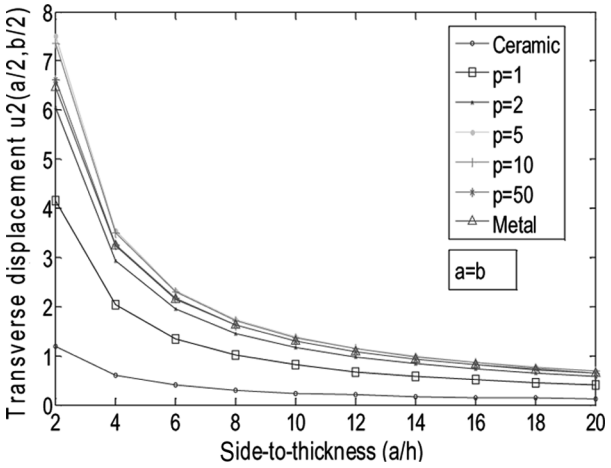

Figure 5 Nondimensional transverse displacement ($\bar{u}_2$) versus side-to-thickness ratio (a/h) of SFGP for different values of grading index (p) under uniformly distributed load.

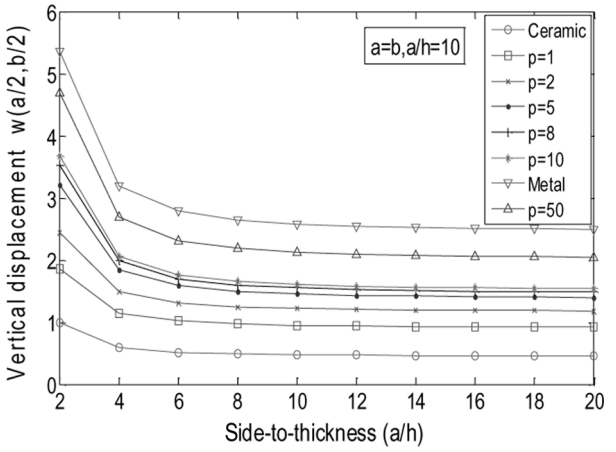

Figure 6 Nondimensional vertical displacement ($\bar{w}$) as a function of side-to-thickness ratio (a/h) of SFGP for different values of grading index (p) under uniformly distributed load.

Figure 5 demonstrates that the transverse displacements for SFGP are not lie in full-metal and full-ceramic plate for some specific values grading index $p = 5$. The slope of transverse displacement is constant when $a/h > 20$.

Figure 6 shows the nondimensional vertical displacement (w) versus thickness variation (x_3/h) for different values of grading index (p).

Figure 6 presents vertical displacement decrease by increasing the values of side-to-thickness. It is seen that slope of decreasing changes to constant values when $a/h > 6$. It is seen that by increasing the value of grading index the vertical displacement increases from smallest value for full-ceramic plate to largest value for full-metal plate.

CONCLUSIONS

The SSDT is successfully applied to present the displacements field in SFGP with simply support conditions subjected to a different type of mechanical loadings such as sinusoidal and uniform distributed loads. The gradation of material properties changes along the thickness direction as simple power law distribution in term of the volume fractions of the constituents. The competed Navire's equations based on SSDT are obtained by using energy method and numerically solved by applying Fourier's series.

Some silence conclusions of this study can be summarized as follows:

- The vertical displacement (deflection, w) decreases with the increase of the aspect ratio whereas the longitudinal stresses ($\bar{\sigma}_{11}$) increase with the aspect ratio decreases for all values of grading index.
- The variation of longitudinal displacement (u_1) is linear through the thickness.
- The transverse displacements in SFGP do not lie between full-ceramic and full-metal plates for some specific values of p ($p = 5$) those results in SFGP are greater than full-metal plate.

- The vertical displacements for SFGP are between full-metal and full-ceramic plate and full-metal plate has the maximum vertical displacement for all values of aspect ratio.
- The vertical displacement decreases with increasing side-to-thickness ratio and the slope gradually becomes constant when $a/h > 6$.

From the presented numerical results it can be suggested that the SSDT have enough accuracy to predict the displacements and in-plane shear stresses in comparison with other shear deformation theories. The out comes of this research can be suggested that the gradation of the constitutive components are a significant parameter in the mechanical responses of SFGP.

REFERENCES

Bahtui, A., Eslami, M. R. (2007). Coupled thermoelasticity of functionally graded cylindrical shells. *Mech. Res. Commun.* 34(1):1–18.

Bayat, M., Sahari, B. B., Saleem, M., Aidy, A., Wong, S. V. (2009). Bending analysis of a functionally graded rotating disk based on the first order shear deformation theory. *Appl. Mech. Model* 33:4215–4230.

Bayat, M., Sahari, B. B., Saleem, M., Ali, A., Wong, S. V. (2008). Thermo elastic solution of a functionally graded variable thickness rotating disk with bending based on the first-order shear deformation theory. *Thin-Walled Struct.* 35:283–309.

Bayat, M., Sahari, B. B., Saleem, M., Hamouda, A. M. S., Reddy, J. N. (2009). Thermo elastic analysis of functionally graded rotating disks with temperature-dependent material properties: uniform and variable thickness. *Int. J. Mechanics and Materials in Design* 5:263–279.

Bayat, M., Saleem, M., Sahari, B. B., Hamouda, A. M. S., Mahdi, E. (2007). Thermo elastic analysis of a functionally graded rotating disk with small and large deflections. *Thin-Walled Struct.* 45:677–691.

Chi, S., Chung, Y. (2006). Mechanical behavior of functionally graded material plates under transverse load – part I: Analysis. *Int. J. Solids Struct.* 43:3657–3674.

Chung, Y.-L., Chen, W.-T. (2007). Bending behavior of FGM-coated and FGM-undercoated plates with two simply supported opposite edges and two free edges. *Comput. Struct.* 81:157–167.

Ebrahimi, F., Rastgoo, A., Kargarnovin, M. H. (2008). Analytical investigation on axisymmetric free vibrations of moderately thick circular functionally graded plate integrated with piezoelectric layer. *J. Mech. Sci. Tech.* 22:1058–1072.

Ferreira, A. J. M., Batra, R. C., Roque, C. M. C., Qian, L. F., Martins, PALS. (2005). Static analysis of functionally graded plates using third-order shear deformation theory and meshless method. *Comp. Struct.* 69:449–457.

Gilhooley, D. F., Batra, R. C., Xiao, J. R., McCarthy, M. A., Gillespie, Jr. JW. (2007). Analysis of thick functionally graded plates by using higher-order shear and normal deformable plate theory and MLPG method with radial basis functions. *Comput. Struct.* 80:539–552.

Howell, A., Bereny, J. (1979). *Engineer's Guide to Solar Energy*. USA: Solar Energy Information Services.

Khdeir, A. A., Reddy, J. N. (1999). Free vibrations of laminated composite plates using second-order shear deformation theory. *Comp. Struct.* 71:617–626.

Matsunaga, H. (2009). Stress analysis of functionally graded plates subjected to thermal and mechanical loadings. *Comput. Struct.* 87:344–357.

Prakash, T., Singha, M. K., Ganapathi, M. (2009). Influence of neutral surface position on the nonlinear stability behavior of functionally graded plates. *Comput. Mech.* 43:341–350.

Praveen, G. N., Reddy, J. N. (1998). Nonlinear transient thermoelastic analysis of functionally graded ceramic-metal plates. *Int. J. Solids Struct.* 35(33):4457–4476.

Qian, L. F., Batra, R. C., Chen, L. M. (2004). Static and dynamic deformations of thick functionally graded elastic plates by using higher-order shear and normal deformable plate theory and meshless local Petrov–Galerkin method. *Composites, Part B* 35:685–697.

Ravikiran, K., Kashif, A., Ganesan, G. (2008). Static analysis of functionally graded beams using higher order shear deformation theory. *Appl. Math. Model* 32:2509–2525.

Reddy, J. N. (2000). Analysis of functionally graded plates. *Int. J. Numer. Meth. Eng.* 47:663–684.

Reddy, J. N. (2007). *Theory and Analysis of Elastic Plates and Shells*. New York: CRC Press.

Reddy, J. N., Cheng, Z.-Q. (2001). Three-dimensional thermo-mechanical deformations of functionally graded rectangular plates. *Eur. J. Mech. A/Solids* 20:841–855.

Sahraee, R. (2009). Bending analysis of functionally graded sectorial plates using Levinson plate theory. *Comp. Struct.* 88:548–557.

Shao, Z. S., Ma, G. W. (2008). Thermo-mechanical stresses in functionally graded circular hollow cylinder with linearly increasing boundary temperature. *Comput. Struct.* 83:259–265.

Sohn, K. J., Kim, J. H. (2009). Nonlinear thermal flutter of functionally graded panels under a supersonic flow. *Comp. Struct.* 88:380–387.

Suresh, S., Mortensen, A. (1998). *Fundamentals of Functionally Graded Materials*. London: IOM Communications Limited.

Yang, J., Shen, H. S. (2003). Nonlinear bending analysis of shear deformable functionally graded plates subjected to thermo-mechanical loads under various boundary conditions. *Composites Part B* 34:103–115.

Yang, Y. Y., Munz, D. (1997). *Stress Analysis in A Two Materials Joint With a Functionally Graded Material*. Elsevier Science B.V.

Zenkour, A. M. (2007). Benchmark trigonometric and 3-D elasticity solutions for an exponentially graded thick rectangular plate. *Arch. Appl. Mech.* 77:197–214.

Zenkour, A. M. (2006). Generalized shear deformation theory for bending analysis of functionally graded plates. *Applied Mathematical Modeling* 30:67–84.